
Figures and figure supplements

Contrary neuronal recalibration in different multisensory cortical areas

Fu Zeng et al.

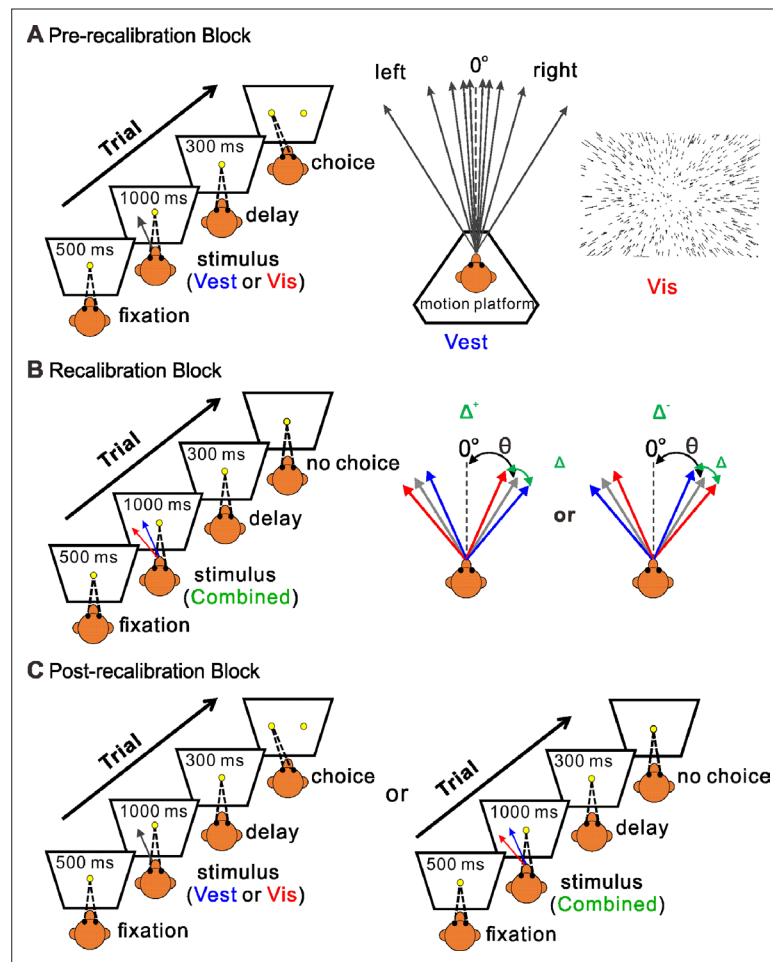


Figure 1. Multisensory recalibration paradigm. **(A)** Pre-recalibration block. The vestibular stimulus was elicited by moving the motion platform (schematic in the middle, viewed from above). The visual stimulus, presented on the screen in front of the monkey, corresponded to optic flow (schematic on the right) as it would be experienced during self-motion (without motion of the platform). The self-motion stimuli comprised linear motions (of either vestibular or visual stimuli) in a forward motion with a small leftward or rightward component (black arrows, schematic in the middle). Monkeys were required to fixate on a central target (yellow circle) presented on the screen during the stimulus and then to report their perceived heading by making a saccade to one of two targets (left or right relative to straight ahead). The heading angle (θ) was varied across trials. **(B)** Recalibration block. Simultaneous vestibular and visual stimuli (combined) with a systematic discrepancy (Δ) between the vestibular and visual headings were presented. Only one discrepancy orientation (Δ^+ or Δ^-) was used per session. The blue and red arrows represent the vestibular and visual headings, respectively. The gray arrows represent the headings (varied across trials) from which the vestibular and visual cues were offset (to either side by $\Delta/2$). The black dashed lines represent straight ahead. **(C)** Post-recalibration block. The single-cue trials (like in A) were interleaved with combined-cue trials (like in B).

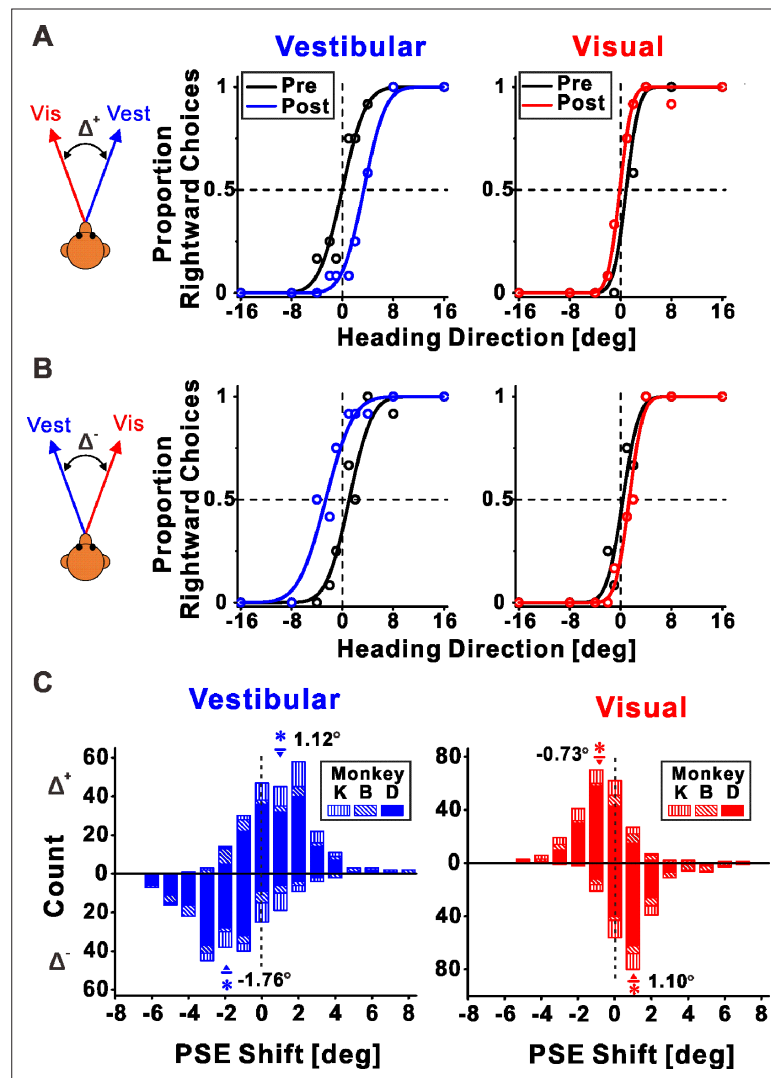


Figure 2. Multisensory recalibration behavior. (A, B) Perceptual recalibration in two example sessions, with (A) Δ^+ (vestibular and visual headings offset to the right and left, respectively; monkey D, session #10) and (B) Δ^- (vestibular and visual headings offset to the left and right, respectively; monkey D, session #48). Psychometric curves (cumulative Gaussian distribution functions) were fitted to the data (circles), and represent the proportion of rightward choices, as a function of stimulus heading direction. Pre-recalibration heading judgments are depicted by black curves, in the left and right columns for vestibular and visual cues, respectively. After recalibration, vestibular and visual curves (blue and red, respectively) were shifted in relation to the pre-calibration curves. (C) Blue and red histograms represent the distributions of the point of subjective equality (PSE) shifts (post-recalibration minus pre-recalibration PSE) for vestibular and visual cues, respectively. Histograms above and below the abscissa represent sessions with Δ^+ and Δ^- , respectively. Inverted triangles (\blacktriangledown) and upright triangles (\blacktriangle) with error bars represent mean \pm standard error of the mean (SEM) shifts for sessions with Δ^+ and Δ^- , respectively. The numbers on the plots represent the mean PSE shifts. Asterisk symbols indicate significant shifts ($p < 0.05$). For the vestibular cue, $p = 2.3 \times 10^{-17}$, $N = 241$ sessions (Δ^+ condition), and $p = 1.0 \times 10^{-28}$, $N = 227$ sessions (Δ^- condition), paired t-test. For the visual cue, $p = 6.5 \times 10^{-11}$ (Δ^+ condition), and $p = 5.4 \times 10^{-23}$ (Δ^- condition), paired t-test. Summary statistics for the individual animals are presented in **Figure 2—source data 1**.

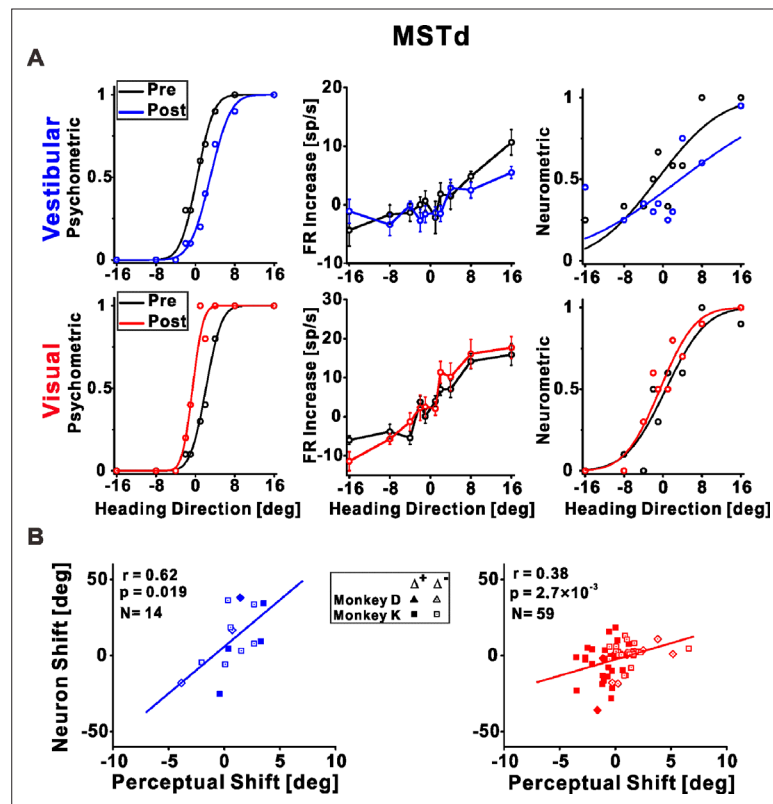


Figure 3. Dorsal medial superior temporal (MSTd) neuronal recalibration. **(A)** An example recalibration session (Δ^+) with simultaneous recording from MSTd. The left column depicts the behavioral responses, pre-, and post-recalibration. The vestibular psychometric curve shifted 3.01° (to the right) and the visual curve shifted -2.71° (to the left). Neuronal responses (middle column) as a function of heading (pre- and post-recalibration). Circles and error bars represent average firing rates (FRs, baseline subtracted) \pm standard error of the mean (SEM). The right column shows corresponding neurometric curves with fitted cumulative Gaussian functions. Each data point shows the proportion of trials in which an ideal observer would make a rightward choice given the FRs of the neurons. The vestibular neuronal shift was 4.73° (to the right) and the visual neuronal shift was -1.22° (to the left). **(B)** Correlations between neuronal point of subjective equality (PSE) shifts and perceptual PSE shifts for the vestibular and visual cues (left and right plots, respectively). Only neurons that passed screening (had significant responses and reliable neurometric PSEs, see Methods for details) were included in this analysis. Solid symbols represent sessions with Δ^+ and open symbols represent Δ^- . The solid lines illustrate the regression lines of the data. r , Pearson's correlation coefficient. Summary statistics for the individual animals, and linear mixed model (LMM) results, are presented in **Figure 3—source data 1** and **Figure 3—source data 2**, respectively.

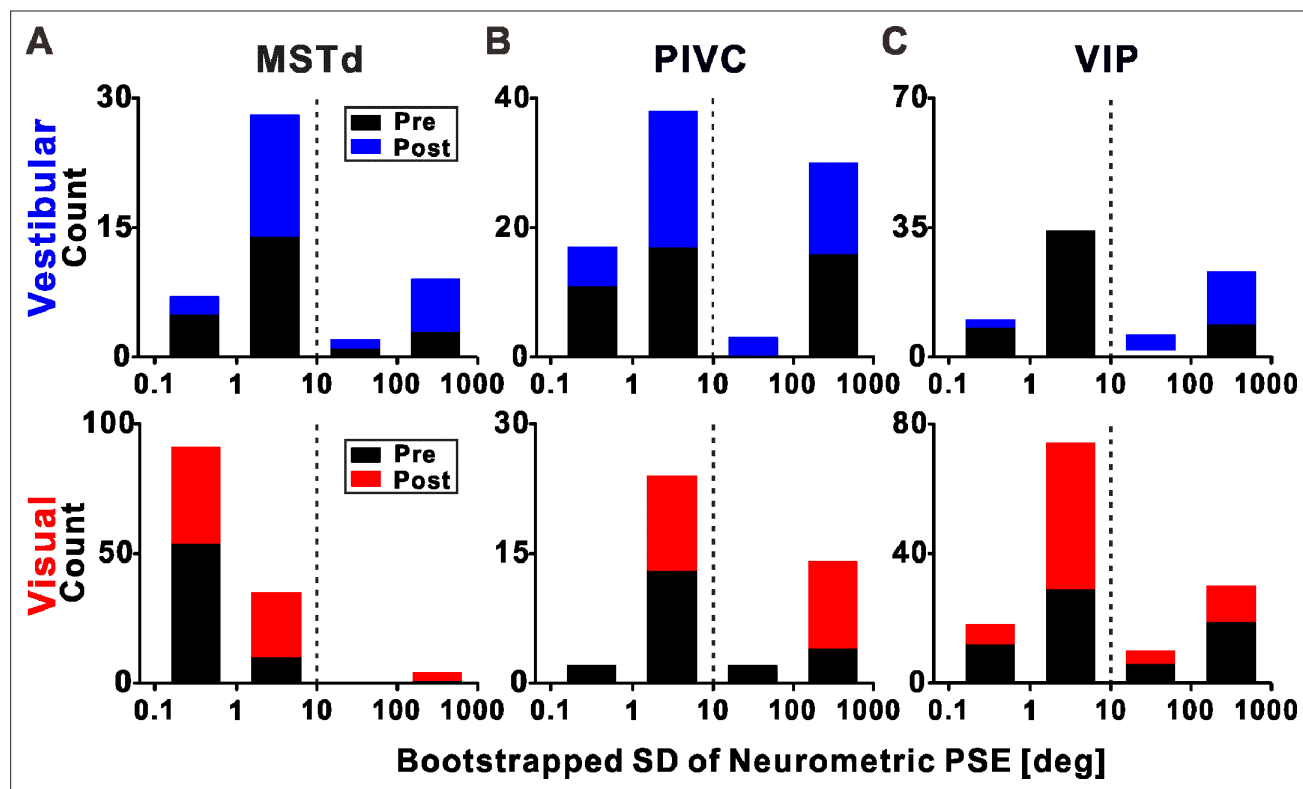


Figure 3—figure supplement 1. Distribution of neurometric point of subjective equality (PSE) reliability. Standard deviations (SDs) of the neurometric PSEs (calculated via bootstrapping) for vestibular and visual stimuli (top and bottom rows, respectively) are presented for neurons recorded from (A) dorsal medial superior temporal (MSTd), (B) parietoinsular vestibular cortex (PIVC), and (C) ventral intraparietal (VIP). Only neurons with significant tuning in the pre- or post-recalibration blocks ($p < 0.05$, Pearson correlation between firing rate and heading) were included here. The vertical dashed lines mark $SD = 10^\circ$. Neurons with an unreliable PSE estimate ($SD > 10^\circ$, in either the pre- or post-recalibration blocks) were excluded from subsequent analyses.

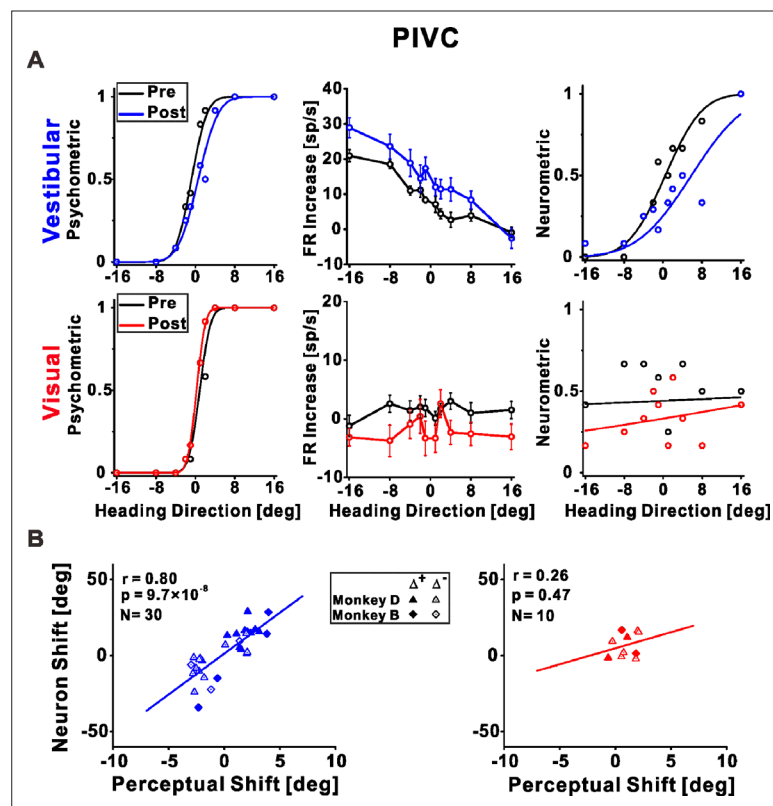


Figure 4. Parietoinsular vestibular cortex (PIVC) neuronal recalibration. **(A)** An example recalibration session (Δ^+) with simultaneous recording from PIVC (conventions are the same as **Figure 3**). The vestibular and visual psychometric curves shifted 1.37° and -0.51° (to the right and left, respectively). The vestibular neurometric curve shifted 5.37° (to the right). Although a visual neurometric curve is presented for this example, no visual neurometric shift was calculated, and the neuron was excluded from subsequent visual cue analyses, because it did not pass the screening for significant tuning to visual stimuli. **(B)** Correlations between neuronal point of subjective equality (PSE) shifts and perceptual PSE shifts for the vestibular and visual cues. Summary statistics for the individual animals, and linear mixed model (LMM) results, are presented in **Figure 4—source data 1** and **Figure 4—source data 2**, respectively.

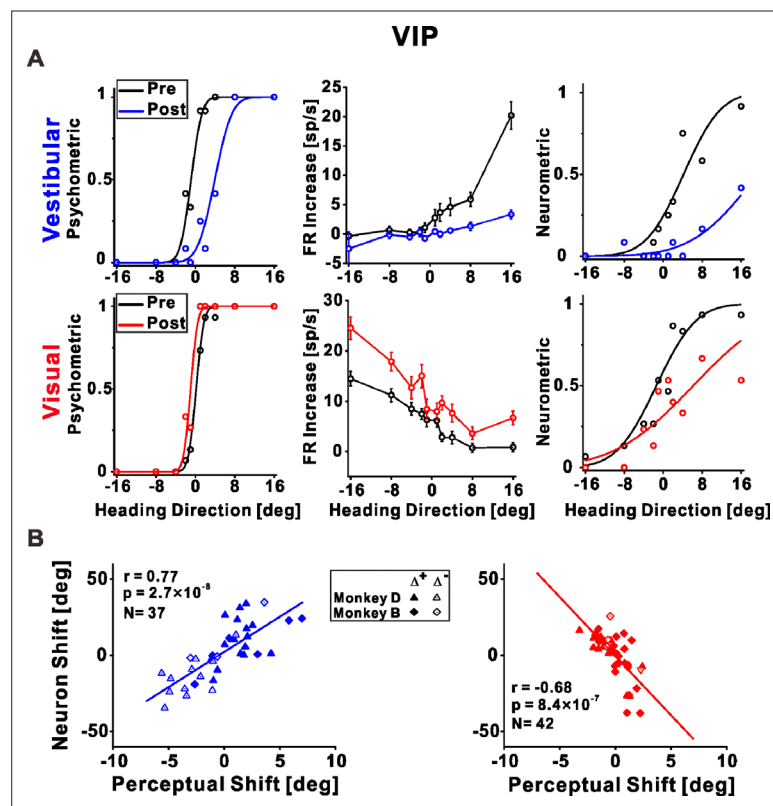


Figure 5. Ventral intraparietal (VIP) neuronal recalibration. (A) An example recalibration session (Δ^+) with simultaneous recording from VIP (conventions are the same as **Figure 3**). The vestibular and visual psychometric curves shifted 4.81° and -1.13° (to the right and left, respectively). The vestibular and visual neurometric curves shifted 15.18° and 7.58° , respectively (both to the right). (B) Correlations between neuronal point of subjective equality (PSE) shifts and perceptual PSE shifts for the vestibular and visual cues. Summary statistics for the individual animals, and linear mixed model (LMM) results, are presented in **Figure 5—source data 1** and **Figure 5—source data 2**, respectively.

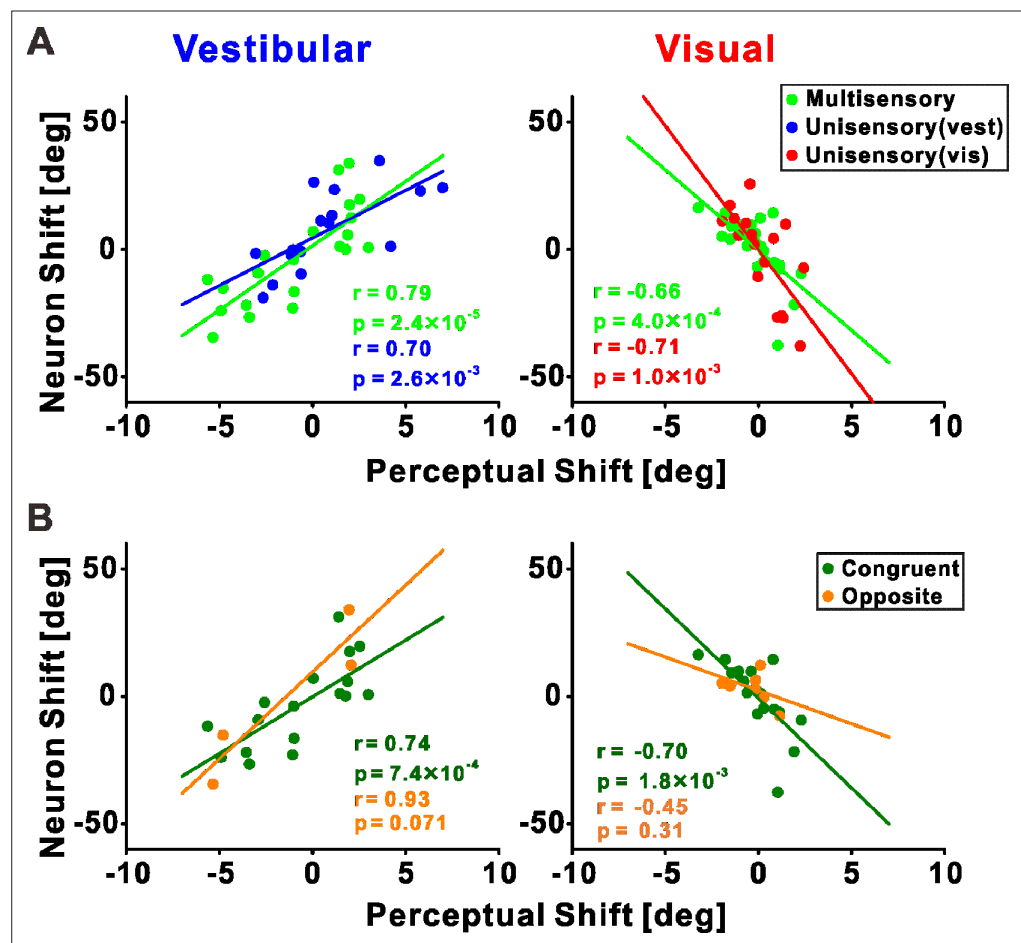


Figure 5—figure supplement 1. Neuronal vs. behavioral shifts by neuron type in area ventral intraparietal (VIP). (A) Neurons with multisensory (green) and unisensory (blue and red, for vestibular and visual, respectively) tuning. (B) Multisensory neurons with congruent (dark green), or opposite (orange), vestibular and visual tuning. The neuronal shifts were positively correlated with the behavioral shifts for the vestibular cue (left column), and negatively correlated with the behavioral shifts for the visual cue (right column). Pearson correlation coefficients are presented on the corresponding plots.

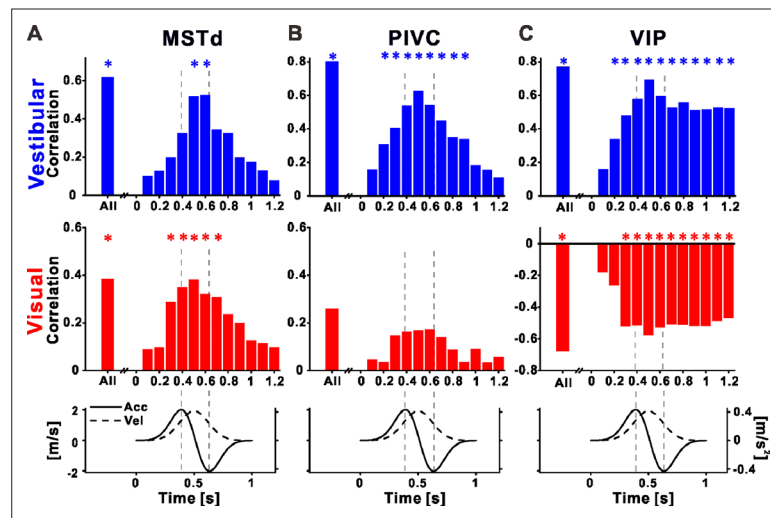


Figure 6. Recalibration of neuronal responses within the stimulus time course. Pearson correlations between neuronal and perceptual point of subjective equality (PSE) shifts, using the neuronal activity at specific time points during the stimulus, for (A) dorsal medial superior temporal (MSTd), (B) parietoinsular vestibular cortex (PIVC), and (C) ventral intraparietal (VIP). Top row: vestibular (blue histograms), middle row: visual (red histograms), bottom row: stimulus (acceleration and velocity) time course. Vertical dashed lines mark peak acceleration and peak deceleration. '*' symbols mark significant correlations.

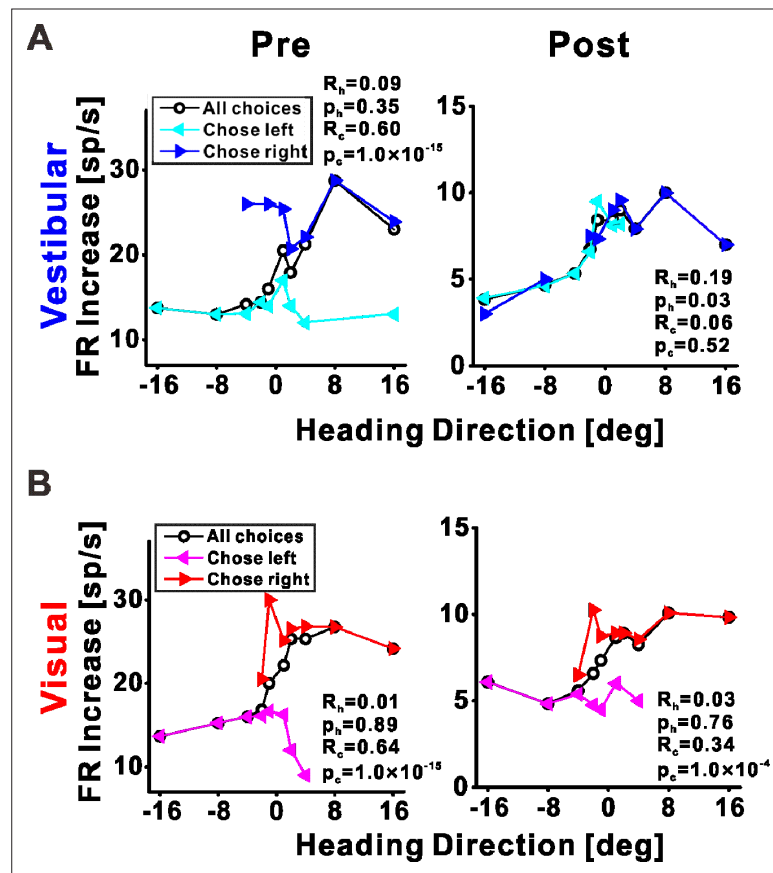


Figure 7. Choice tuning is reduced post-recalibration in an example ventral intraparietal (VIP) neuron. Neuronal responses for an example VIP neuron to (A) vestibular and (B) visual heading stimuli, pre- and post-recalibration (left and right columns, respectively). Blue and cyan curves depict choice-conditioned tuning curves (neuronal responses followed by rightward and leftward choices, respectively) for the vestibular cue. Red and magenta curves depict choice-conditioned tuning curves for the visual cue. Black curves (in the corresponding plots) represent all responses (not sorted by choice). Partial heading (R_h) and partial choice (R_c) correlations (with corresponding p values) are presented on the plots.

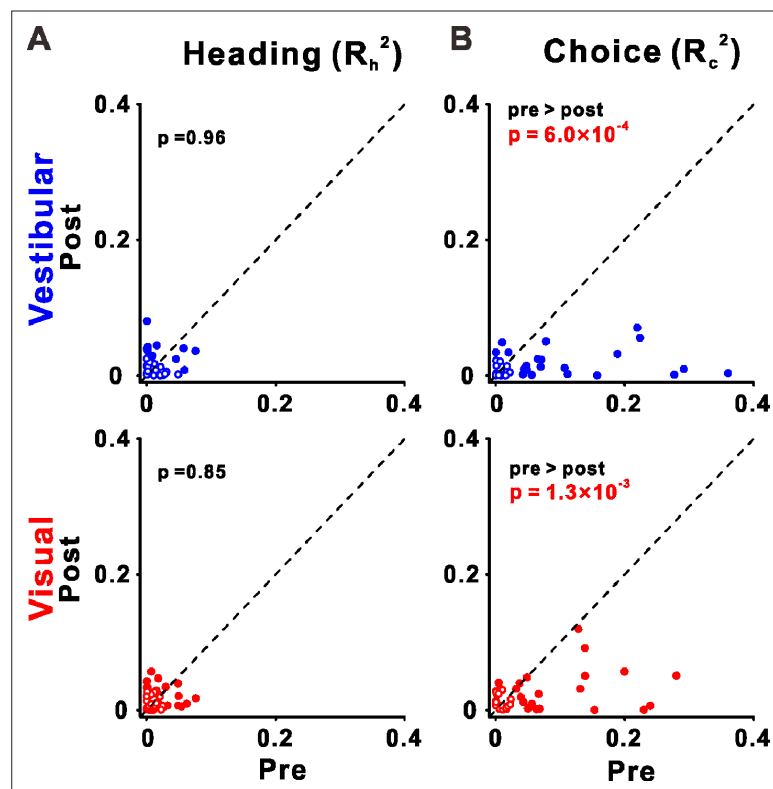


Figure 8. Choice tuning is reduced in ventral intraparietal (VIP) post-recalibration. (A) Heading and (B) choice partial correlation coefficients (squared) are depicted post- vs. pre-recalibration. Blue and red circles (top and bottom rows) represent vestibular and visual cues, respectively. Filled (empty) circles indicate significant (non-significant) partial correlations for heading or choice. p values are presented on the corresponding plots (two-tailed paired t-tests).

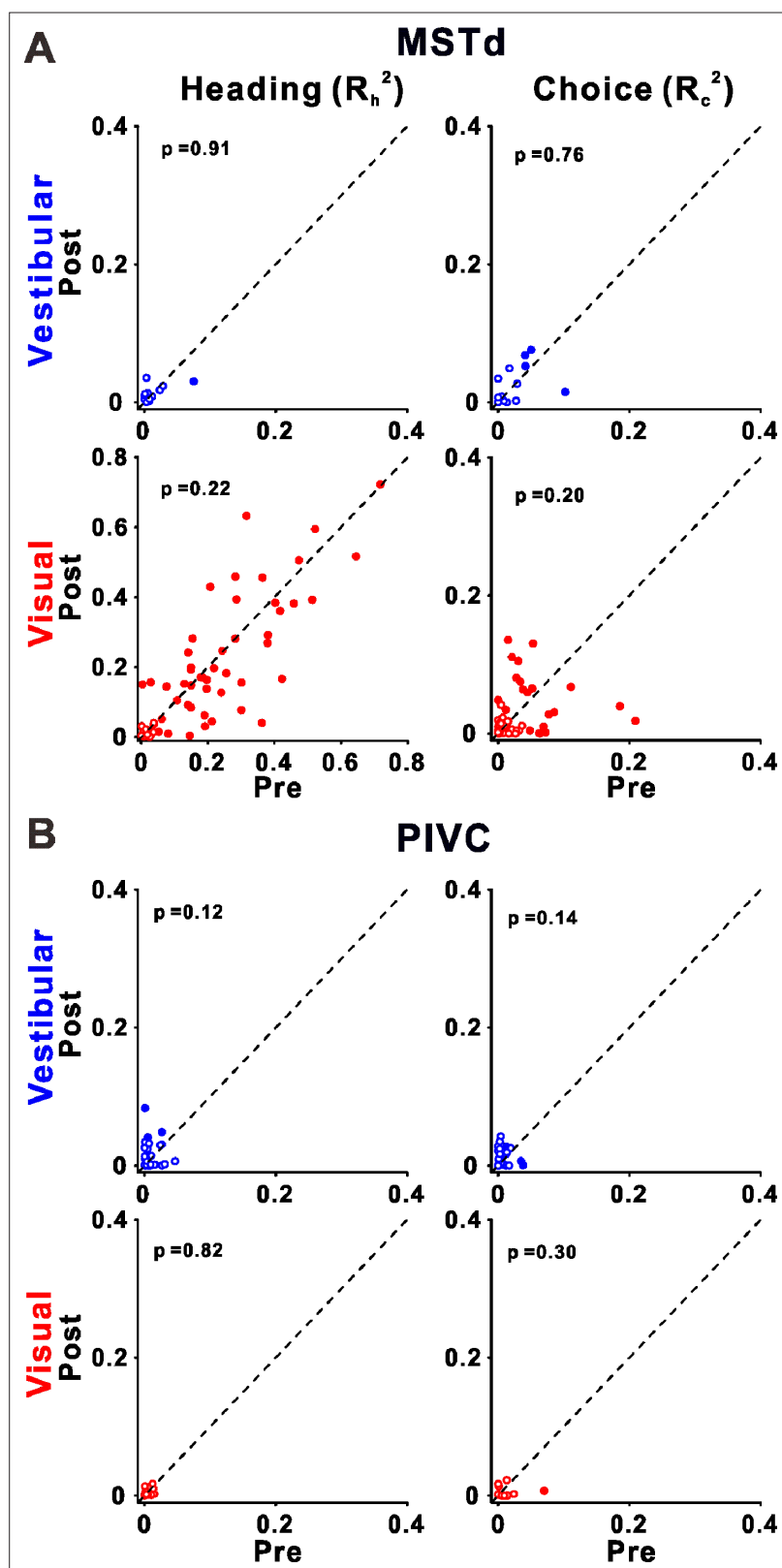


Figure 8—figure supplement 1. Choice and heading partial correlations. (A) Dorsal medial superior temporal (MSTd) and (B) parietoinsular vestibular cortex (PIVC). Plotting conventions are the same as **Figure 8**.

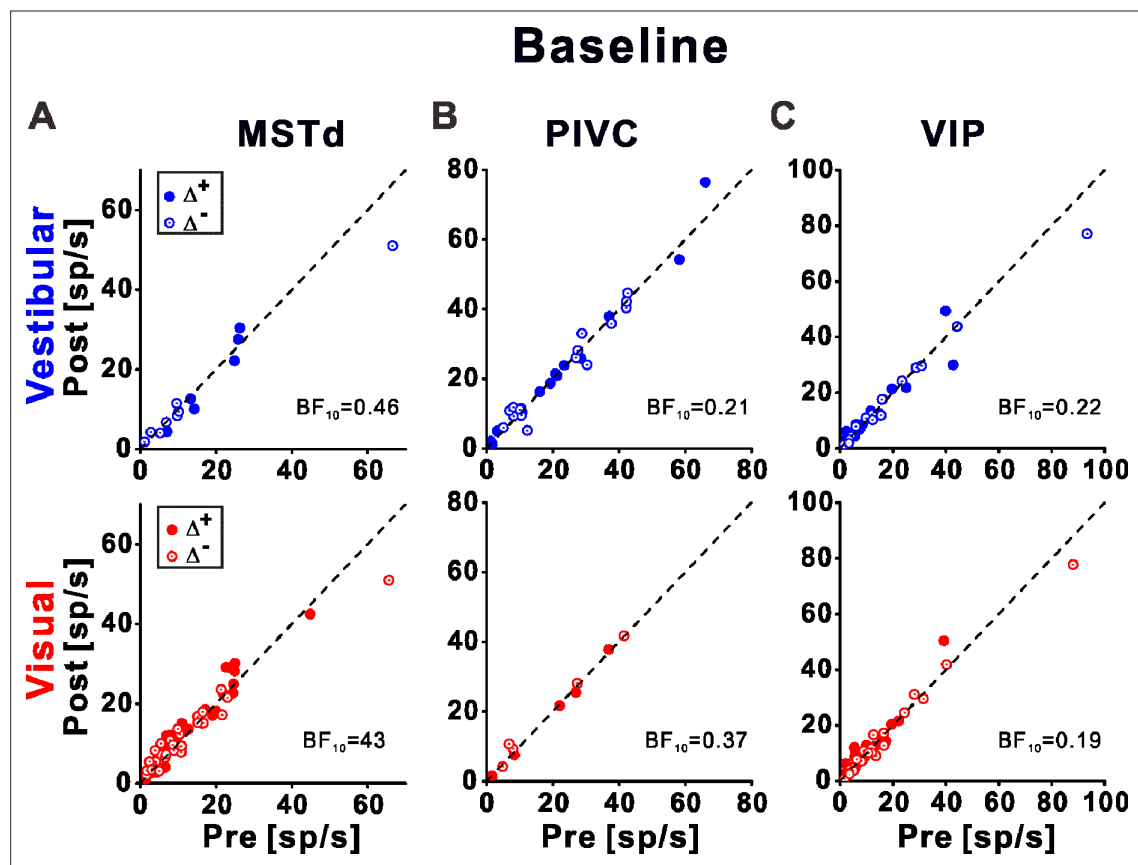


Figure 8—figure supplement 2. Baseline firing rates. The post- vs. pre-recalibration baseline firing rates in areas (A) dorsal medial superior temporal (MSTd), (B) parietoinsular vestibular cortex (PIVC), and (C) ventral intraparietal (VIP) are plotted for vestibular and visual cues (top and bottom rows, respectively). Solid symbols represent Δ^+ and open symbols represent Δ^- . Bayes factors (BF_{10}) $< \frac{1}{3}$ (as for PIVC vestibular cue and VIP) provide substantial evidence against a change in baseline firing rates. Bayes factors between $\frac{1}{3}$ and 3 (as for MSTd and PIVC visual cues) are inconclusive (provide no substantial evidence for, or against, changes).